JOURNAL OF NANO- AND ELECTRONIC PHYSICS
Vol. **9** No 6, 06005(4pp) (2017)

ЖУРНАЛ НАНО- ТА ЕЛЕКТРОННОЇ ФІЗИКИ
Том **9** № 6, 06005(4cc) (2017)

New Optimized Intermediate Band (IB) Design to Improve ZnTeO Solar Cell Performances

B. Lakehal[1,2], Z. Dibi[2], N. Lakhdar[3]

[1] *Department of Electronics, University of Kasdi Merbah Ouargla, 30000 Ouargla, Algeria*
[2] *LAAAS Laboratory, University of Batna1, 05000 Batna, Algeria*
[3] *Department of Electrical Engineering, University of El Oued, 39000 El Oued, Algeria*

(Received 02 July 2017; revised manuscript received 15 November 2017; published online 24 November 2017)

In this paper, a genetic algorithm-based approach is proposed to extract and optimize the design parameters of the intermediate band solar cell (IBSC) in order to improve the electrical performance and the conversion efficiency behavior of the device. The proposed approach is applied to investigate the effect of the energy level (E_i) intermediate band (IB) and electronic states density (Ni) influence on cell efficiency. The presented analytical models are used as objective functions, which are required for our optimization approach. The obtained results are compared with analytical results found in literature indicating the applicability of the genetic algorithm technique to study the electrical behavior of the IBSC design. Therefore, this approach will be extended to alternative solar cell for motivating experimental efforts to realize these promising photovoltaic devices.

Keywords: Intermediate band, Genetic algorithms, Optimization, Conversion efficiency.

DOI: 10.21272/jnep.9(6).06005 PACS numbers: 85.55.De, 84.60.Jt

1. INTRODUCTION

The possibility for increasing the efficiency of photovoltaic solar cells via sequential absorption of photons in a single material has a relatively long history [1]. The concept of multiband or intermediate band solar cell (IBSC) identify the three possible photon absorption mechanisms [2-4]. Several approaches have been proposed to practically realize an IBSC, including quantum dots, impurity doping and dilute semiconductor alloys [5]. Theoretically it is possible to go beyond the Shockley-Queisser efficiency limit with IB materials. An example of the bulk IB materials is oxygen doped ZnTe (ZnTe:O) [6-8].

The intermediate band solar cell (IBSC)-based design is used to provide a better performances compared with those of single gap solar cells by using the energy of sub-band-gap energy photons [9, 10], characterized by the existence of an intermediate band (IB) located in the forbidden gap between the conduction and valence bands (CB and VB), respectively [9]. This IB should be half-filled with electrons (metallic) in order to provide both empty states to receive electrons from the VB as well as electrons to supply to the CB [10]. Therefore, the intermediate band is responsible for the simultaneous absorption of two below band-gap energy photons which demonstrated a significant improvement in photocurrent and efficiency in the solar cell. In other hand, photons with less energy than the one necessary to pump an electron from the VB to the CB can be absorbed by transitions that pump an electron from the VB to the IB were also capable of pumping electrons from the IB to the CB. Thus, a full VB → CB electron transition (also called electron-hole pair generation) can be completed by means of two photons of energy below the band-gap [11-13].

In this context, the main objective of this work is to propose an approach based on Genetic Algorithms for maximizing the photovoltaic conversion of the IBSC-based design. The genetic algorithm-based approach is used for optimizing the geometrical and physical parameters of the device design in order to improve electrical behavior and show the effect of the energy position for IB on the cell performances. The results obtained are compared to analytical ones found in literature makes our approach an alternative solution to the designer to choose the best device design for high-cell performances.

2. MODELING METHODOLOGY

Genetic algorithms are biological process search by population, impelled by Darwin's theories of evolution and also the conception of 'survival of the fittest'. Genetic Algorithms use processes analogous to genetic recombination and mutation to market the evolution of a population that best satisfies a predefined goal [14]. Given a large collection of potential solutions to the given problem and by evaluating how well each solution solves the problem, genetic operators (mutation, crossover) are applied to create a new generation of solutions. In our study the baseline photocurrent density of the structure ZnTeO based IBSC for optical transitions from the valence band to the conduction band, The schematic structure of ZnTe-based IBSCS is presented in Fig. 1. Material parameters for ZnTe are chosen in this analysis as a prototypical material for IBSC due to recent interest in oxygen-doped ZnTe as an active region for IBSC devices.

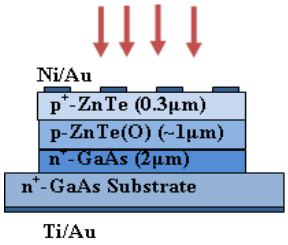

Fig. 1 – Intermediate band solar cells structure

Implementation of GA needs the determination of six elementary issues: chromosome representation

(population), genetic operators (mutation, crossover), initialization, selection function, termination and evaluation function (fitness function). Therefore, the flow diagram of genetic algorithm is presented in Fig. 2 [15, 16].

The baseline photocurrent density due to valence band VB to conduction band CB optical transitions for this device structure may be expressed as

$$J_{ph} = J_{L0} D\left[1 - exp\left(-1/D\right)\right], \quad (1)$$

$$D = \left(\tau_{n,tot}\mu_n F + \tau_{p,tot}.\mu_p F\right)\left(1 - V_a / V_{bi}\right)/W, \quad (2)$$

where J_{L0} is the photocurrent density at large reverse bias, W is the width of the absorber $\tau_{n,tot}$ and $\tau_{p,tot}$ are the total recombination lifetime values for electrons and holes, μ_n and μ_p are the mobility of electrons and the mobility of holes, respectively. F represents the electric field. is given by [12, 19]

The photon carrier generation rates and absorption coefficients of different transitions as a function of energy are expressed follows :

$$G_{\mathrm{IC}}(x) = \int_{E_i}^{E_c} a_{\mathrm{IC}}(E) I_{\mathrm{li}}(E) \exp\left(-a_{\mathrm{tot}}(E)x\right) dE, \quad (3)$$

$$G_{\mathrm{VI}}(x) = \int_{E_V}^{E_i} a_{\mathrm{VI}}(E) I_{\mathrm{li}}(E) \exp\left(-a_{\mathrm{tot}}(E)x\right) dE. \quad (4)$$

Furthermore, with supposed the net recombination lifetime and optical absorption coefficients are linear relationships depending on the cross sections for optical absorption ($\sigma_{opt,n}$ and $\sigma_{opt,p}$) and the electronic states density of IB (N_i) [20]:

$$\alpha_{IC}(Ni) = \alpha_{IC0} f = \sigma_{opt,n} N_i f, \quad (5)$$

$$\alpha_{VI}(Ni) = \alpha_{VI0}(1-f) = \sigma_{opt,p} N_i f, \quad (6)$$

$$\tau_{tot}(Ni) = 1/C_p N_i, \quad (7)$$

where C_p is the capture coefficient, f represents filling of intermediate band.

The I_{li} Indicates solar spectrum as a function of energy is given by [20]:

$$I_{\mathrm{li}}(E) = X f_s \frac{2\Pi}{h^3 C^2} \frac{E^2}{\exp\left(\frac{E}{KT_s}\right) - 1}, \quad (8)$$

where X is concentration of the solar, f_s = 1/46050 is the solid angle under the sun, T_s = 5963 K is the sun temperature, K refers to the Boltzmann constant, C is the speed of light and h is the Planck constant.

The total current density in this structure are the sum of dark and photocurrent current density due to VB, CB and IB radiative transitions.

$$J = J_D - \left(J_{ph} + J_{ph;IB}\right), \quad (9)$$

where J_D represents the dark current density. As a function of the densities of the following currents such as the diffusion current J_{diff}, the radiative current density ($J_{r,CV}$), current density due to the intermediate band of radiative recombination is ($J_{r,CI}$) and the current density of non radiative recombination Jnr. are given by the following expressions[23]:

$$J_D = J_{diff} + J_{r,CV} + J_{r,CI} + J_{nr}, \quad (10)$$

$$J_{\mathrm{diff}} = \left(\frac{qn_i^2 D_n}{W_p N_D} + \frac{qn_i^2 D_p}{W_n N_A}\right)\left(\exp\left(\frac{qV_a}{KT}\right) - 1\right), \quad (11)$$

$$J_{r,\mathrm{CV}} = q\frac{2\Pi}{h^3 C^2}\int_{E_g}^{\infty} E^2\left(1 - \exp\left(Wa_{\mathrm{vc}}\right)\right)\exp\left(\frac{-E}{KT}\right)dE \times \times\left(\exp\left(\frac{qV_a}{KT}\right) - 1\right), \quad (12)$$

$$J_{r,\mathrm{CI}} = \left(q\frac{2\Pi}{h^3 C^2}\int_{E_i}^{E_c} E^2\left(1 - \exp\left(Wa_{Ic}\right)\right)\exp\left(\frac{-E}{KT}\right)dE\right) \times \times\left(\exp\frac{qV_a(1-\xi)}{KT} - 1\right), \quad (13)$$

$$J_{nr} = \frac{qn_i W}{2\tau_{tot}\gamma}\left(\exp\left(\frac{qV_a}{KT}\right) - 1\right), \quad (14)$$

where V_a is the applied bias refers to the bias voltage, W_n and W_p are the widths of the n and p-type, respectively. N_A and N_D are the acceptor and donor concentration, respectively. ni represents the intrinsic carrier concentration, D_n and D_p are the electron and hole diffusion coefficients, respectively, ξ is a value between 0 and 1 under dark conditions, γ = 10.

The power conversion efficiency of the solar cell is calculated as:

$$\eta = \frac{P_{\max}}{P_s} = \frac{\mathrm{FF}.J_{sc}.V_{oc}}{P_s}, \quad (15)$$

where J_{sc} is the short circuit current density, V_{oc} is the open circuit voltage, FF is the fill factor, P_s is the incident power. P_{max} the maximum power from the solar cell.

3. GA-BASED OPTIMIZATION

In this work, the optimization process is based on genetic algorithm in order to solve complex problems by exploring all regions of state space and using different genetic operators such as: selection, crossover and mutation, which will be applied to individuals in populations [27]. In this context, we consider an initial population size of 100 individuals where each of them contains a set of four parameters which are $N_A = N_D$, $a_{IC0} = a_{VI0}$, W et τ_{tot}.

Considering previous analytical model [12], these parameters are confined within a given range shown by the following Table. 1.

A tournament selection is employed which selects each parent by choosing individuals at random, and then choosing the best individual out of that set to be a parent. Scattered crossover creates a random binary vector. A maximum number of generations equal to 300, for which stabilization of the fitness function was obtained.

Table 1 – Description of the special paragraph styles

Parameters	Values
$N_A = N_D$	10^{14} to 10^{21} cm^{-3}
$\alpha_{IC0} = \alpha_{VI0}$	100 to 10^4 cm^{-1}
W	100 nm to 10 um
τ_{tot}	1 to 100 us

The flowchart of our proposed GA-based approach to find the appropriate optimal parameters is shown in Fig. 2.

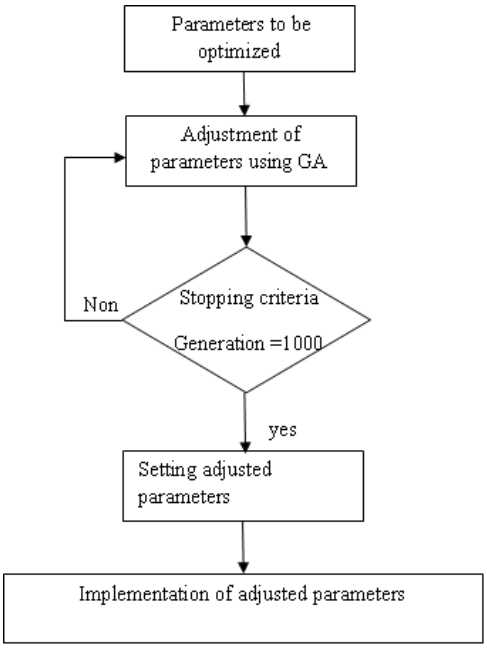

Fig. 2 – Flowchart of our GA-based approach

4. RESULTS AND DISCUSSION

In this work, we propose an approach based on GA computation to optimize the electrical behaviour of the IBSC-based design. In order to minimize equation (15), routines from GA toolbox in MATLAB 7.2 are used. Therefore, various configuration parameters for optimization mentioned above are also used. Table 2 summarizes the optimized IBSC design parameters. It is clearly shown that an improvement in the conversion efficiency

Table 2 – Comparison between analytical [12] and optimized results of IBSC design for various electrical and photovoltaic parameters

Parameters	Analytical results [12]	Optimized IBSC design
N_A[cm^{-3}]	10^{19}	1.72×10^{20}
N_D[cm^{-3}]	2×10^{18}	1.72×10^{20}
α_{IC0}[cm^{-1}]	10^4	9.65×10^3
α_{VI0}[cm^{-1}]	10^4	9.65×10^3
τ_{tot}[us]	1	9.72
W[um]	1	1.5
J_{sc}(mA/cm^2)	17.22	17.71
V_{oc}(V)	1.825	1.825
FF	0.922	0.923
η(%)	28.96	29.877

of the optimized IBSC design has been found in comparison with the analytical model of the same structure [12].

Fig. 3 shows the calculated current-voltage characteristics of the analytical model presented in literature [12] and our optimized approach. Good agreement between the optimized model results and analytical model ones found in literature is obtained. It is noticed that the optimized IBSC design demonstrates a better electrical behavior. This improvement can be explained by the applicability of GA technique to study the IBSC performances.

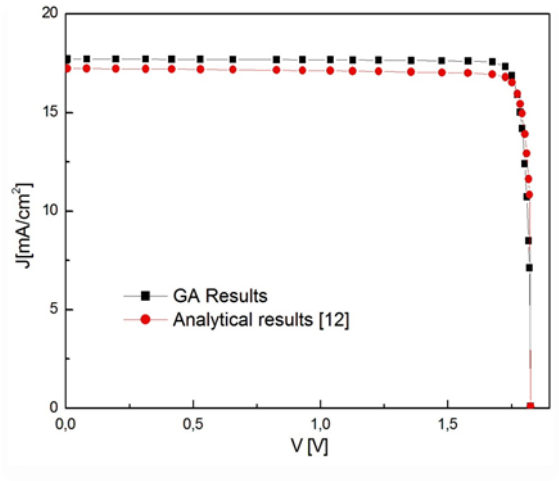

Fig. 3 – Calculated I-V characteristics of the IBSC design

The variation of current-voltage characteristics of the IBSC-based design of the analytical and GA results with different absorption coefficients are shown in Fig 4. It is observed that the short circuit current density J_{sc} increases with increased of α_{IC0} and α_{VI0}. However, the open circuit voltage V_{oc} does not change with the variation of α_{IC0} and α_{VI0}. The increase in J_{sc} over the baseline cell (the case of $\alpha_{IC0} = \alpha_{VI0} = 0$) is explained by the sub band gap photon absorption.

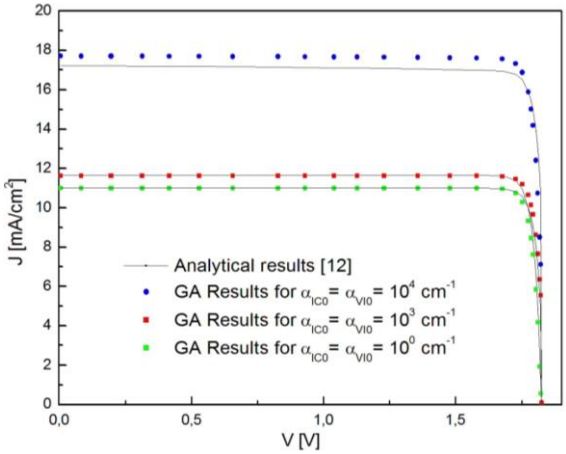

Fig. 4 – Variation of I-V characteristics of the IBSC design with different absorption coefficients

The effect of the energy level (E_i) on the performance of the solar cell is illustrated in Fig. 5. It is noticed that the increasing in the energy position (IB) from 0.4 to 0.6 eV, the efficiency increases slightly from 14.91 % to its

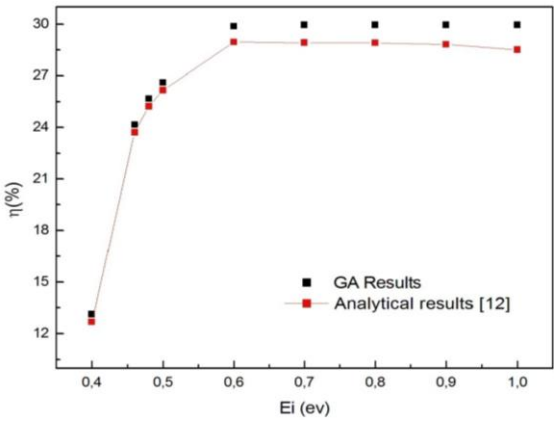

Fig. 5 – Variation of efficiency versus the energy level (E_i)

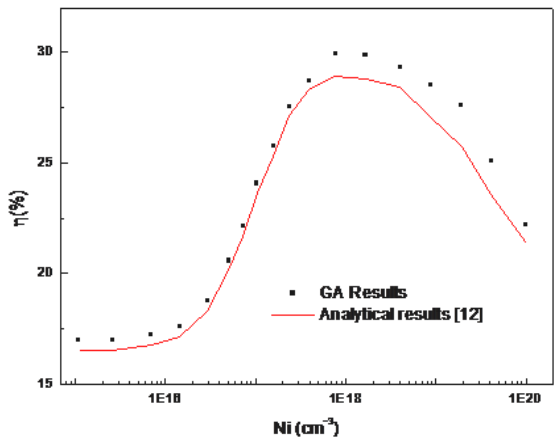

Fig. 6 – Variation of the efficiency versus the electronic states density Ni

maximum value 28.97 % and will be stabilized even as the energy position increases.

Fig. 6 shows a comparison between a calculated efficiency using GA-based approach and analytical results as function as the electronic states density (Ni) of the IBSC design. It is observed that a better efficiency can be found when the electronic states density increases from 10^{15} cm^{-3} to 10^{18} cm^{-3}. However, it degrades gradually when electronic states density continues to increase. This is can be explained by the impact of the electronic states density on the optical absorption and the recombination process properties.

Therefore a quantitative understanding of these relationships is necessary for a specific IBSC model. Furthermore, the effect of Ni on the IBSC performance can be determined by using the capture coefficient and cross sections as described in equations (5, 7). For this study we have proposed the values of 10^{-13} cm^{3}s^{-1} and 10^{-16} cm^2 for the capture coefficient and the cross sections, respectively.

5. CONCLUSION

This work focused particularly on the study of IBSC design. In this context, an approach based on genetic algorithms has been developed in order to increase the photovoltaic conversion of device. The influence of various parameters on the conversion efficiency has been illustrated in order to predict desirable characteristics before elaborating them. Therefore, the proposed structure is based on optimization of physical and geometrical parameters which directly affect the electrical behavior to improve the performances of IBSC design. It has been found that a significant improvement is evidenced by our GA-based approach compared to analytical results providing an alternative structure to designer for future applications.

REFERENCES

1. Y. Okada, N.J.E. Daukes, T. Kita, R. Tamaki, M. Yoshida, A. Pusch, O. Hess, C.C. Phillips, D.J. Farrell, K. Yoshida, N. Ahsan, Y. Shoji, T. Sogabe, J.-F. Guillemoles, *Appl. Phys. Lett.* **2**, 021302 (2015).
2. T. Tanaka, K.M. Yu, P.R. Stone, J.W. Beeman, O.D. Dubon, L.A. Reichertz, V.M. Kao, M. Nishio, W. Walukiewicz, *Appl. Phys. Lett.* **108**, 024502 (2010).
3. W. Wang, A.S. Lin, J.D. Phillips and W.K. Metzger, *J. Appl. Phys. Lett.* **95**, 261107 (2009).
4. A. Martí, E. Antolín, C.R. Stanley, C.D. Farmer, N. López, P. Díaz, E. Cánovas, P. G. Linares, A. Luque, *Phys. Rev. Lett.* **97**, 247701 (2006).
5. C. Ling, L.Q. Zhou, D. Banerjee, H. Jia, *J. Alloy. Compd.* **584**, 289 (2014).
6. T. Tanaka, Y. Nagao, T. Mochinaga, K. Saito, Q. Guo, M. Nishio, K.M. Yu, W. Walukiewicz, *J. Cryst. Growth* **378**, 259 (2013).
7. Y. Shoji, K. Akimoto, Y. Okada, *J. Phys. D* **46**, 024002 (2013).
8. A. Martí, N. López, E. Antolín, E. Cánovas, and A. Luque C.R. Stanley, C.D. Farmer, P. Díaz, *Appl. Phys. Lett.* **90**, 233510 (2007).
9. A. Martí, E. Antolín, E. Cánovas, N. López, P.G. Linares, A. Luque, C.R. Stanley, C.D. Farmer, *Thin Solid Films* **516**, 6716 (2008).
10. A. Luque, A, Marti, *Adv. Mater.* **22**, 160 (2007).
11. B. Lakehal, Z. Dibi, N. Lakhdar, A. Dendouga, *Sādhanā. Springer* **40**, 1473 (2015).
12. A.S. Lin, W. Wang, J.D. Phillips, *J. Appl. Phys.* **105**, 064512 (2009).
13. W. Wang, A.S. Lin, J.D. Phillips, *J. Appl. Phys.* **95**, 011103 (2009).
14. D.W. Boeringer, D.H. Werner, *IEEE. T Anten Propag.* **52**, 771 (2004).
15. J. Robinson, S. Sinton, Y. Rahmat-Samii, *IEEE Antennas Propagat. Soc. Int. Symp. Dig.* **01**, 314 (2002).
16. B. Brandstatter, U. Baumgartner, *IEEE T. Magn.* **38**, 997 (2002).
17. W. Wang, A. Lin, J.D. Phillips, *J. Electron. Mater.* **37**, 1044 (2008).
18. A. Luque, A. Martí, N. López, E. Antolín, E.C.C. Stanley, C. Farmer, P. Díaz, *J. Appl. Phys.* **99**, 094503 (2006).
19. A. Luque, A. Martí, *Phys. Rev. Lett.* **78**, 5014 (1997).
20. G. Wei, K.T. Shiu, N.C. Giebink, S.R. Forrest, *Appl. Phys. Lett.* **91**, 223507 (2007).
21. A. Luque, A. Marti, *Prog in Photovoltaics.* **9**, 73 (2001).
22. L. Cuadra, A. Martí, A. Luque, *IEEE T. Electron Dev.* **51**, 1002 (2004).
23. N. Lakhdar, F. Djeffal, *Microelectron. Reliab.* **52**, 958 (2012).